CANCER GENOMICS & PROTEOMICS *10*: 251-264 (2013)

Rho Kinase Proteins Regulate Global miRNA Expression in Endothelial Cells

JESSICA M. STILES, VITTAL KURISETTY, DIANNE C. MITCHELL and BRAD A. BRYAN

Department of Biomedical Sciences, Texas Tech University Health Sciences Center, El Paso, TX, U.S.A.

Abstract. *Background: Therapeutic targeting of Rho-Associated, Coiled-Coil Containing Protein Kinase (ROCK) signaling for tumor cells and tumor endothelium has shown efficacy in pre-clinical tumors models, and a better understanding of how proteins regulate tumor progression will strengthen our knowledge over disease etiology and treatment of patients with cancer. Recent reports have shown that ROCK activity is critical for the expression of a large number of mRNA transcripts across multiple cell types including endothelial cells. Materials and Methods: To examine the effects of ROCK proteins on microRNA (miRNA) expression in tumor-forming endothelial cells, we utilized microarrays to evaluate expression levels of 1088 miRNAs in vascular tumor-forming endothelial cells knocked-down for ROCK1 or ROCK2 or treated with a pharmacological inhibitor of ROCK activity. Results: Microarray analysis demonstrated that inhibiting ROCK activity altered global miRNA expression. We confirmed our findings using qPCR and identified cell-cycle progression, calcium transport, and neurogenesis/synaptogenesis as the most highly overrepresented predicted target gene networks for the identified miRNAs whose expression was altered by ROCK inhibition. Conclusion: ROCK signaling induces large-scale changes in global miRNA expression and may lead to a better understanding of how these proteins affect aberrant vascular states.*

The small GTPase RhoA and its downstream serine/threonine kinase effectors Rho-kinase 1 &2 (ROCK1 &2) are involved in a diverse array of biological processes affecting organismal development and disease states *via* regulating the actin cytoskeleton and associated signaling networks. Over the past two decades, the primary focus of researchers studying the roles of ROCK1 & 2 has been centered on the coordinative control of the actin cytoskeleton and cell movement by these proteins. Particular interest has been placed on elucidating and pharmacologically-exploiting their role in motility, invasion, and metastasis in tumor cells (1), however new insights into the functions of the ROCK proteins suggest that targeting ROCK's kinase activity in the tumor stroma may lead to increased treatment efficacy (2). For instance, publications from our laboratory and others have focused heavily on the roles of the ROCK proteins in vascular biology, demonstrating clearly that ROCK activity is essential for endothelial cell function in both normal and aberrant states. ROCK2[+/–] mice display decreased expression of endothelial cell markers in their lungs (3) and inhibition of ROCK signaling effectively disrupts vascular endothelial growth factor (VEGF)-mediated endothelial cell differentiation and activation (3-8). The enhanced ability of tumor-derived endothelial cells to organize into *in vitro* vascular networks is dependent on ROCK activity (9) and shRNA-mediated knockdown of ROCK expression in angiosarcoma models leads to significant reductions in tumor volume (4). Thus, further expansion of our knowledge on how ROCK signaling mediates normal and aberrant endothelial processes could assist in understanding how targeting these proteins modulates tumor progression and metastasis as well as a wide range of vascular diseases.

As changes in cytoskeletal dynamics and cell morphology are intimately-involved in the regulation of global gene expression (10), it is logical to presume that ROCK protein's phosphorylation of key cytoskeletal regulators may indirectly or directly alter the global gene expression profile of the cell. A handful of studies have shown that the kinase activity of ROCK proteins dramatically influences the expression of the transcriptome at a global level in a number of cell types including endothelial cells (11-14). Furthermore, shRNA-mediated knockdown of ROCK expression is capable of negating a large percentage of VEGF-induced gene expression in endothelial cells (4). While these studies have

Correspondence to: Brad A. Bryan, Texas Tech University Health Sciences Center, Paul L. Foster School of Medicine, Center of Excellence in Cancer Research, 5001 El Paso Drive, MSB1 Room 2111, El Paso, Texas 79905 U.S.A. Tel: +1 9152154232, Fax: +1 9157835222, e-mail: brad.bryan@ttuhsc.edu

Key Words: Rho kinase, ROCK, endothelial cell, angiogenesis, tumor vasculature, shRNA, miRNA, microarrays.

focused on the effects of ROCK inhibition at the messenger RNA level, it has been reported that ROCK activity regulates the oncomir miR-17-92 in breast tumors potentially *via* modulation of Myc signaling (15). Similar to its broad reaching effects on global mRNA transcriptional expression, this suggests that ROCK activity may also affect the steady state level of any number of miRNAs.

It is possible that ROCK-mediated inhibition of endothelial network formation and vascular tumor progression is due, in part, to altered expression of miRNAs. To address this issue and further understand the role of ROCK proteins in the global regulation of aberrant endothelial miRNAs, we utilized shRNA technology to knock-down the expression of ROCK1 &2 in vascular tumor-forming endothelial cells and performed miRNA expression microarrays to identify differentially expressed miRNAs whose steady-state levels were dependent on ROCK activity.

Materials and Methods

Cell lines and treatments. The transformed mouse endothelial line MS1 (MILE SVEN 1) was purchased from the American Type Culture Collection (ATCC, Rockville, MD, USA). Cells were grown at 37˚C in a 5% CO_2 humidified incubator using Dulbecco's modified Eagle's medium (DMEM) supplemented with 10% fetal bovine serum and penicillin/streptomycin. MS1 cells were transfected *via* Lipofectamine 2000 (Invitrogen, Carlsbad, CA, USA) with plasmids (SABiosciences, Valencia, CA, USA) containing the shRNA sequences *GCGCAATTGGTAGAAGAATGT* for ROCK1 knock-down or *AACCAACTGTGAGGCATGTAT* for ROCK2 knock-down. These sequences were previously shown by our laboratory to effectively knock-down ROCK1 and ROCK2 in the MS1 cell line (4). As a control, MS1 cells were transfected with a plasmid (SABiosciences, Valencia, CA, USA) containing the scrambled sequence *GGAATCTCTCATTCGATGCATAC*. Cell pools were stably-selected with hygromycin. To ablate the kinase activity of both ROCK1 and ROCK2, we treated cells for 24 h with 10 μM Y-27632, a competitive inhibitor of ATP binding to the kinase domain of both ROCK1 and ROCK2 (16).

Total RNA isolation. Total RNA was extracted using the mirVana miRNA Isolation Kit (Applied Biosystems, Foster City, CA, USA) according to the manufacturer's instructions.

miRNA microarray and data analysis. miRNA microarray analysis for 1088 miRNAs was performed in triplicate using the miRNA One Array Mouse V3 (Phalanxbiotech; Belmont, CA, USA) with Cy3 label according to the manufacturer's directions. The microarrays were scanned using an Axon GenePix 4400A (Molecular Devices, Sunnyvale, CA, USA). Background signal was subtracted and samples were normalized using GeneSpring v12.5. miRNAs reported as differentially expressed possessed a *p*-value less than 0.05 (Student's *t*-test) with a change of at least two-fold above or below the control (scrambled shRNA) sample. Predicted target genes for the miRNAs of interest were obtained from MicroRNA Target Prediction and Functional Study Database (MIRDB) (www.mirdb.org). Process network maps for the predicted miRNA target genes were statistically ranked using Metacore software (Thompson-Reuters, New York City, NY, USA). Direct and indirect functional interaction maps for the predicted miRNA target genes were generated using String (www.string-db.org). Venn diagrams were created using an online gene list Venn diagram generator (http://simbioinf.com/mcbc/applications/genevenn/genevenn.htm) (17).

Quantitative real-time polymerase chain reaction (qPCR). miRNA was amplified using the TaqMan miRNA Reverse Transcription Kit (Applied Biosystems, Foster City, CA, USA) and a miRNA-specific stem-looped RT primer according to the manufacturer's instructions. TaqMan miRNA assays specific to each differentially expressed miRNA of interest were employed to measure the levels of selected miRNAs *via* qPCR on an ABI7900HT real time PCR instrument (Invitrogen, Carlsbad, CA, USA). Each reaction was performed in triplicate. Relative miRNA expression data were analyzed using the ΔΔCt method (18).

Results

MS1 miRNA expression profile. The MS1 cell line is a previously isolated transformed endothelial line that has been used to study benign vascular tumor formation and tumor angiogenesis (19). Injection of these cells into nude mice leads to the development of small non-progressive tumors with prominent stroma. The tumors grow to a maximum size of approximately 2 mm^3 and remain stable throughout the life of the host. Though MS1 endothelial cells have served as an important model for studying tumor angiogenesis, the global miRNA expression profile of this cell line has not been previously documented and may reflect the miRNA patterns indicative of aberrant endothelial cells such as the tumor endothelium. The raw data collected from our microarray analysis of 1,088 mouse miRNAs in the MS1 endothelial cell line revealed that signal intensities for each miRNA varied widely with a range of 30±6 to 2,5881±1,120 (Table I), indicating that the MS1 cell line possesses a unique miRNA expression pattern. Out of the 1,088 mouse miRNAs tested, 52% (563) of miRNAs were detected at significant levels (defined as signal intensity greater than 500 units) and 48% (525) exhibited no to low signal (defined as signal intensities less than 500 units) (Figure 1A and B). These results suggest that approximately half of the total miRNA population is expressed to some degree in MS1 cells. Of particular interest, 56 miRNAs were highly expressed in the MS1 cell line with signal intensities greater than 20,000 units. Among all 1,088 analyzed miRNAs, the top five miRNAs exhibiting the highest expression included miR-1894-5p, miR-1952, miR-149*, miR-877*, and miR-3102*.

shRNA-mediated knockdown of ROCK expression levels alters the miRNA profiles of endothelial cells. To investigate the roles of ROCK proteins on the global miRNA expression profile of endothelial cells, we utilized shRNA-mediated knockdown of ROCK 1 & 2 levels in MS1 endothelial cells. As demonstrated

Table I. *miRNA Expression for MS1 endothelial cells*.

Signal intensity	Number	miRNAs
>20,000	56	miR-1894-5p, miR-1952, miR-149*, miR-877*, miR-3102*, miR-1943*, miR-207, miR-328*, miR-5127, miR-1224*, miR-574-5p, miR-669c*, miR-504*, miR-1188*, miR-664, miR-466f-3p, miR-3082-5p, miR-466i-5p, miR-874*, miR-667, miR-760-5p, miR-1224, miR-2183, miR-5109, miR-532-3p, miR-3102-3p.2, miR-705, miR-1249*, miR-711, miR-3473d, miR-5132, miR-3100-3p, miR-210*, miR-3968, miR-296-3p, miR-3070a*,miR-3070b-5p, miR-1187, miR-466c-5p, miR-18b*, miR-1247*, miR-762, miR-467f, miR-494, miR-690, miR-669f-5p, miR-466m-5p, miR-669m-5p, miR-5107, miR-466i-3p, miR-466h-3p, miR-5110, miR-3057-3p, miR-466j, miR-669l, miR-669e, miR-328, miR-7b*
10,000-20,000	96	miR-466f, miR-1894-3p, miR-709, miR-466q, miR-3960, miR-669a-5p, miR-669p, miR-3473b, miR-667*, miR-92a-2*, miR-1897-5p, miR-5115, miR-669c, miR-466h-5p, miR-468, miR-3100-5p, miR-30c-1*, miR-1892, miR-669a-3p,miR-669o-3p, miR-1188, miR-1940, miR-764-5p, miR-7a-2*, miR-129-2-3p, miR-3087*, miR-672, miR-669k*, miR-466m-3p, miR-1905, miR-297a, miR-1895, miR-483, miR-5113, miR-698, miR-466f-5p, miR-2137, miR-574-3p, miR-466g, miR-3099*, miR-1195, miR-669o-5p, miR-129-1-3p, miR-1192, miR-669n, miR-150, miR-2182, miR-1966, miR-3077*, miR-1982*, miR-466k, m-3b, miR-3090*, miR-669b, miR-92b*, miR-3102-5p.2, miR-320, miR-3064-5p, miR-1306-5p, miR-3104-5p, miR-877, miR-669d, miR-467d*, miR-5128, miR-669p*, miR-1934*, miR-744, miR-346*, miR-3099, miR-467b*, miR-706, miR-466d-5p, miR-3107,miR-486, miR-1946a,miR-1946b, miR-5126, miR-1896, miR-3083*, miR-467h, miR-298, miR-214, miR-3102, miR-696, miR-3473, miR-1196, miR-3097-5p, miR-32*, miR-670, miR-669f-3p, miR-664*, miR-423-5p, miR-710, miR-3472, miR-1943, miR-467a*, miR-467g, miR-466b-5p,miR-466o-5p, miR-1935, miR-1903
5000-9999	45	miR-467c, miR-297a*,miR-297b-3p,miR-297c*, miR-211*, miR-29b-1*, miR-669a-3-3p, miR-1249, miR-297b-5p, miR-1306-3p, miR-3095-3p, miR-2136, miR-702, miR-5099, miR-206, miR-467c*, miR-297c, miR-365-1*, miR-210, miR-1934, miR-760-3p, miR-674, miR-1198-5p, miR-5105, miR-1967, miR-1186b, miR-30c-2*, miR-1907, miR-467e*, miR-3103*, miR-23a*, miR-669e*, miR-3470b, miR-3072*, miR-466o-3p, miR-21, miR-1902, miR-694, miR-466a-5p,miR-466p-5p, miR-669b*, miR-5134, let-7b, miR-26a-2*, miR-3470a, miR-1931, miR-3076-5p, miR-320*
1000-4999	182	miR-292-3p, miR-466d-3p, miR-5101, miR-204*, miR-193b*, miR-326*, miR-7a, miR-493, miR-3060, miR-466e-5p, miR-669d*,miR-669d-2*, miR-3103, miR-1951, miR-1186, miR-335-3p, miR-3059*, miR-30b*, miR-122, miR-691, miR-3059, miR-1930*, miR-466n-5p, miR-1962, miR-483*, miR-673-3p, miR-669l*, miR-193b, miR-1949, miR-19b, miR-135a-1*, miR-194-2*, miR-452-5p, miR-3474, miR-1982.1,miR-1982.2, miR-5136, miR-3065, miR-200c*, miR-466a-3p,miR-466b-3p,miR-466c-3p,miR-466e-3p,miR-466p-3p, miR-125a-5p, miR-185, miR-29a*, miR-665, miR-674*, miR-16, miR-135a-2*, miR-125b-5p, miR-325, miR-3097-3p, miR-669h-3p, miR-1941-5p, miR-302c, miR-5104, miR-1970, miR-150*, miR-465b-5p, miR-3081*, miR-3070b-3p, miR-152*, miR-187, miR-185*, miR-99b*, miR-324-3p, miR-5116, miR-669i, miR-34c*, miR-1900, miR-1933-3p, miR-3064-3p, miR-363-5p, miR-5118, miR-329, miR-194, miR-125a-3p, miR-3098-3p, miR-222*, miR-9*, miR-1971, miR-432, miR-329*, miR-3096-5p, miR-542-3p, miR-761, miR-467e, miR-218-1*, miR-3091-3p, miR-668*, miR-878-3p, miR-299*, miR-3089-5p, miR-3092, miR-19a, miR-1906, miR-1956, miR-720, miR-5135, miR-449b, miR-383*, miR-3101*, miR-337-5p, miR-494*, miR-669m-3p, miR-485*, miR-3061-5p, miR-3113*, let-7b*, miR-770-3p, miR-669h-5p, miR-680, miR-714, miR-551b*, miR-466l-3p, miR-370, let-7e, miR-297a-5*, miR-693-5p, miR-3098-5p, miR-5114, miR-497, miR-3971, miR-3091-5p, miR-5130, miR-365-2*, miR-190b, miR-3107*,miR-486*, miR-330*, miR-678, miR-1839-5p, miR-365, miR-195*, miR-882, miR-5129, miR-93, miR-542-5p, miR-221*, miR-206*, miR-376b, miR-344d-2*, miR-341, miR-155, miR-410*, miR-675-3p, miR-3572, miR-208a-5p, miR-434-3p, miR-3060*, miR-671-3p, miR-2861, miR-145, miR-138, miR-489, miR-294, miR-758*, miR-16-1*, miR-196b*, miR-670*, miR-721, miR-713, miR-342-5p, miR-327, miR-665*, miR-194-1*, miR-703, miR-344d, miR-15a*, miR-673-5p, miR-1898, miR-1247, miR-330, miR-28*, let-7c, miR-208b*, miR-344d-1*, miR-195, miR-3075, miR-652*, miR-7b, miR-1968, miR-5117, miR-5119, let-7a, miR-1960, miR-5112
500-999	184	miR-344c*, miR-188-5p, miR-181d, miR-1958, miR-677*, miR-3473c, miR-223*, miR-412-3p, miR-34a, miR-1981, miR-1904, miR-196a, miR-654-5p, m-73B, miR-701, miR-679-5p, miR-128-2*, miR-511-5p, miR-764-3p, miR-470, miR-455, miR-3961, miR-338-5p, miR-704, miR-3112*, miR-383, miR-199a-3p,miR-199b, miR-1983, miR-134, miR-5120, miR-1933-5p, miR-133b, miR-192*, miR-125b-1-3p, miR-449a*, miR-3058*, miR-540-3p, miR-3096-3p,miR-3096b-3p, miR-491*, miR-344, miR-448-5p, miR-1941-3p, miR-129-5p, miR-1843b-5p, miR-598*, miR-3106, miR-339-5p, miR-1930, miR-717, miR-666-3p, let-7i, miR-382, miR-376a, miR-681, miR-5100, miR-5106, let-7f, miR-15b, miR-325*, miR-875-3p, miR-568, miR-215, miR-326, miR-298*, miR-3073-3p, miR-200a*, miR-290-3p, miR-211, miR-345-5p, miR-677, miR-10b, miR-141*, miR-323-5p, miR-149, miR-134*, miR-701*, miR-181b, miR-5097, miR-683, miR-1947*, miR-31, miR-3969, miR-224*, miR-695, miR-374*, miR-98, miR-33*, miR-3110, miR-378, miR-34b-3p, miR-1948, miR-3093-3p, miR-547*, miR-1981*, miR-20b, miR-1190, miR-700*, miR-20b*, miR-547, miR-200b*, miR-5123, miR-1936, miR-22*, miR-449c, miR-186, miR-3085-5p, miR-671-5p, miR-615-3p, miR-202-3p, miR-106b, miR-5046, miR-1843-5p, miR-1965, miR-433*, miR-128-1*, miR-5122, miR-135b, miR-450a-2*, miR-92b, miR-184, miR-3475, miR-375*, miR-23a, miR-3087, miR-668, miR-3067, let-7d, miR-18b, miR-501-5p, miR-672*, miR-3065*, miR-335-5p, miR-138-1*, miR-103-2*, miR-148a, miR-1964-3p, let-7d*, miR-376c, miR-539-3p, miR-590-3p, miR-345-3p, miR-105, miR-465a-5p, miR-582-3p, miR-3096b-5p, miR-378*, miR-484, miR-214*, miR-140*, miR-135a, miR-485, miR-719, miR-744*, miR-693-3p, miR-187*, miR-300, miR-1947, miR-497*, miR-1927, miR-343, miR-147*, miR-338-3p, miR-676, miR-24, miR-669g, miR-3057-5p, miR-409-3p, miR-346, miR-1b-5p, miR-339-3p, miR-3110*, miR-143*, miR-1963, miR-133b*, miR-219-3p, miR-675-5p, let-7g*, miR-5131, miR-802*, miR-181d*, miR-499*, miR-378b, miR-505-5p, miR-292-5p

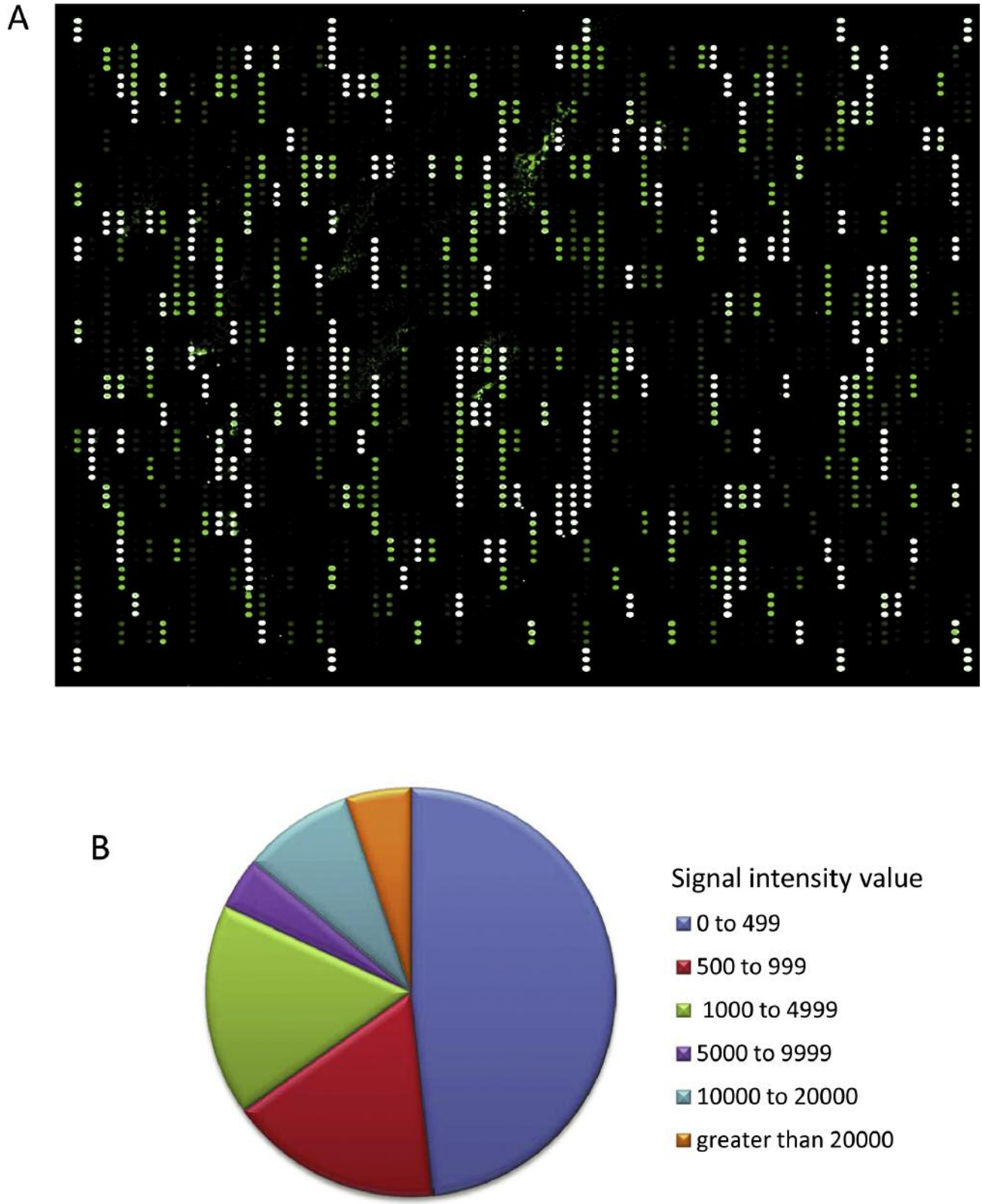

Figure 1. *miRNA expression profile of MS1 endothelial cells. A total of 1,088 mouse miRNAs were analyzed by miRNA microarrays. (A) The expression profile of 1,088 miRNAs in MS1 cells based on the fluorescent scan of the hybridized array. As signal intensity increases, the corresponding color intensity changes from black to green to white. (B) miRNA distribution based on signal intensity in the microarray analysis.*

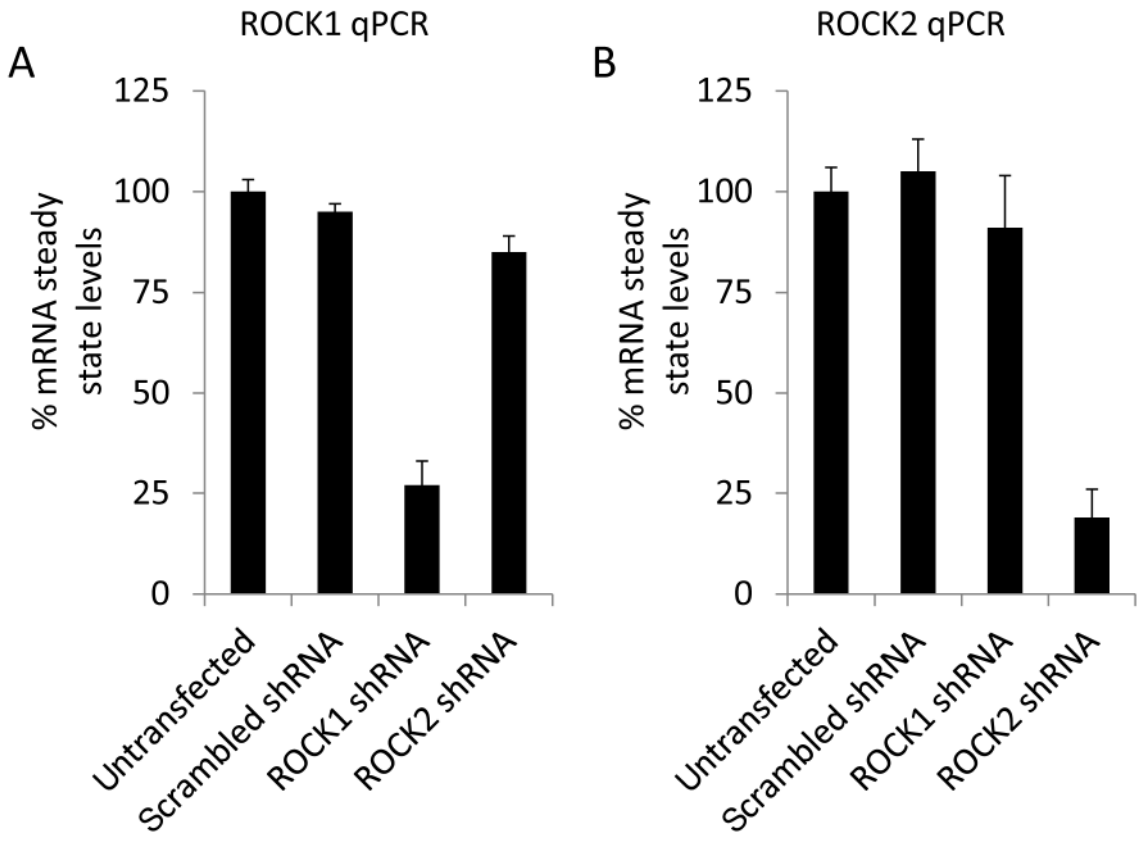

Figure 2. *shRNA-mediated knockdown of ROCK paralogs. MS1 endothelial cells were stably transfected with shRNA plasmids specific against ROCK1 or ROCK2 as well as a scrambled shRNA control. qPCR was performed to determine the levels of ROCK1 and ROCK2 for the scrambled shRNA and ROCK knockdowns relative to the untransfected control. (A) qPCR data for ROCK1 levels. (B) qPCR data for ROCK2 levels.*

in Figure 2, shRNA knockdown of ROCK1 &2 resulted in approximately 75% and 80%, reduction in mRNA levels relative to the scrambled control treated cells, respectively. Cells were grown to confluency, RNA was collected, and miRNA expression arrays were performed to examine the relative levels of miRNAs across the treatments. As an additional experimental variable, the microarrays were performed on scrambled control endothelial cells where the kinase activity of both ROCK proteins was inhibited with the well-established ROCK inhibitor Y27632 (10 μM). This essentially served as a "double-knockout" of both ROCK1 and ROCK2 activity. The miRNA expression pattern of ROCK1 and ROCK2 knockdown and Y-27632-treated endothelial cells was distinctly different from the scrambled control cells. Out of the 1,088 investigated miRNAs, a two-fold or greater change in expression relative to the scrambled control was observed for 269 (118↑, 151↓), 292 (114↑, 178↓), and 290 (121↑, 169↓) miRNAs in the ROCK1 shRNA, ROCK2 shRNA, and Y27632 conditions, respectively (Figure 3; Table II). With few exceptions, ROCK1 and ROCK2 control of global miRNA expression trended in a largely overlapping manner, and these results were corroborated when both ROCK1 and ROCK2 kinase activity was abrogated in the Y27632 treatment. For instance, strict Venn analysis that eliminated all miRNAs with fold changes less than two-fold revealed 106 up-regulated and 131 down-regulated miRNAs, whose expression was shared between the ROCK knockdowns and the Y27632 treatment (Figure 4), though almost the exclusive majority of the miRNA expression changes that did not fall in the commonly-expressed Venn area trended in similar directions between the treatments.

Validation of miRNA expression using qPCR. Verification of the miRNA microarray data was performed for the top four miRNAs whose expression was increased in our microarray analysis relative to the scrambled control in both ROCK knockdowns as well as the Y27632 treatment (mir-1894-5p, mir-764-3p, mir-466f-3p, and mir-669c*). Through qRT-PCR-analyzed fold changes for these miRNAs, we validated the fold changes calculated from the microarray signal data, with each of these miRNAs consistently demonstrating increased steady-state expression levels relative to the control (Figure 5).

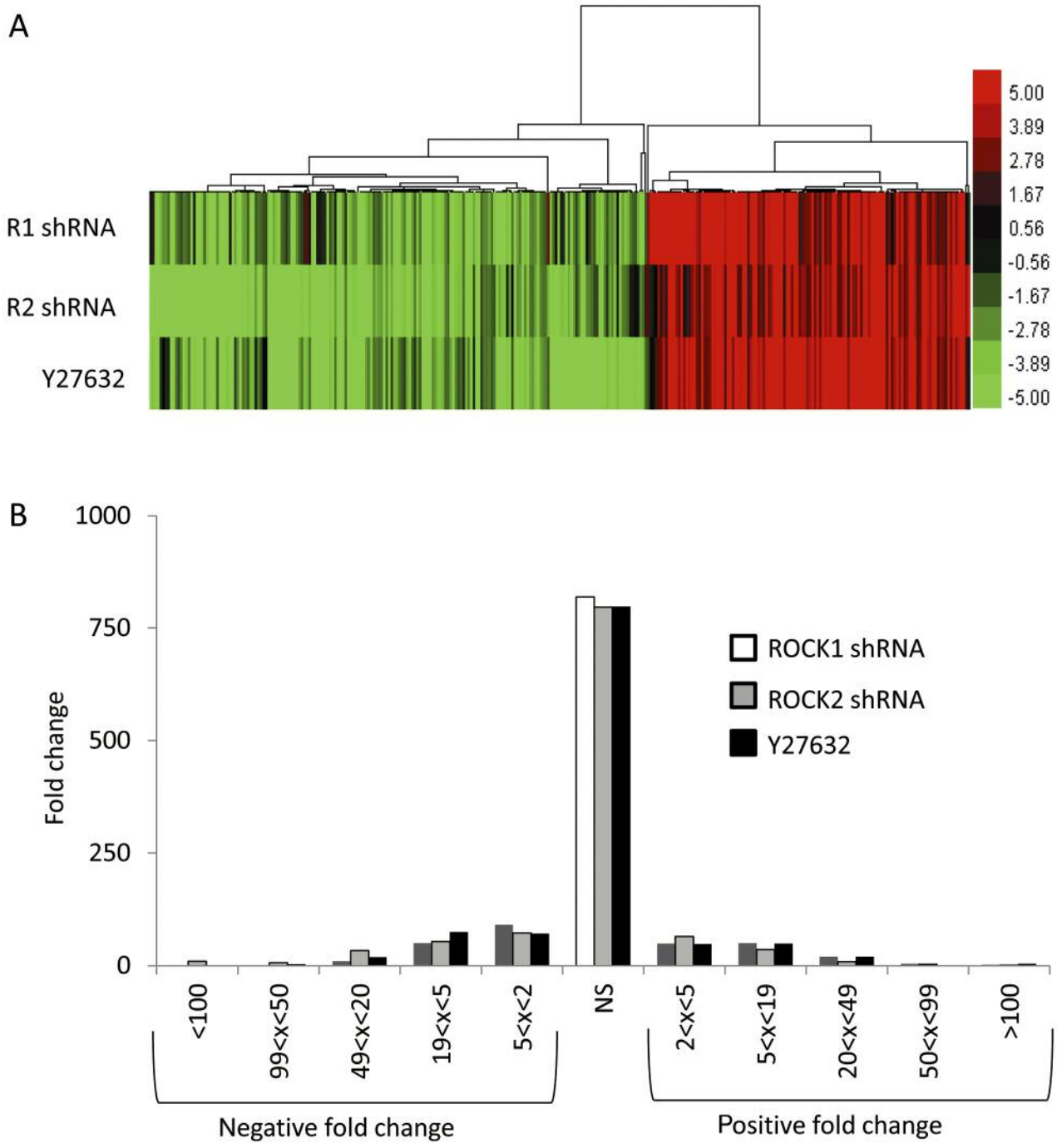

Figure 3. *ROCK-mediated alterations in miRNA expression. (A) Hierarchical-clustered heatmap illustrating the two-fold or greater miRNA expression changes in MS1 cells knocked-down for ROCK1 or ROCK2, or treated for 24 h with 10 μM Y27632 relative to the scrambled shRNA control. (B) miRNA fold change distribution for MS1 cells knocked-down for ROCK1 or ROCK2, or treated for 24 h with 10 μM Y27632 relative to the scrambled shRNA control.*

Network analysis of miRNA signaling pathways. To understand the potential effects of ROCK-mediated regulation of miRNA expression in endothelial cells, we performed *in silico* network analysis on mir-1894-5p, mir-764-3p, mir-466f-3p, and mir-669c* which were all commonly up-regulated in both the microarray and qPCR validation for ROCK1 shRNA, ROCK2 shRNA- or Y27632-treated endothelial cells. We utilized the MicroRNA Target Prediction

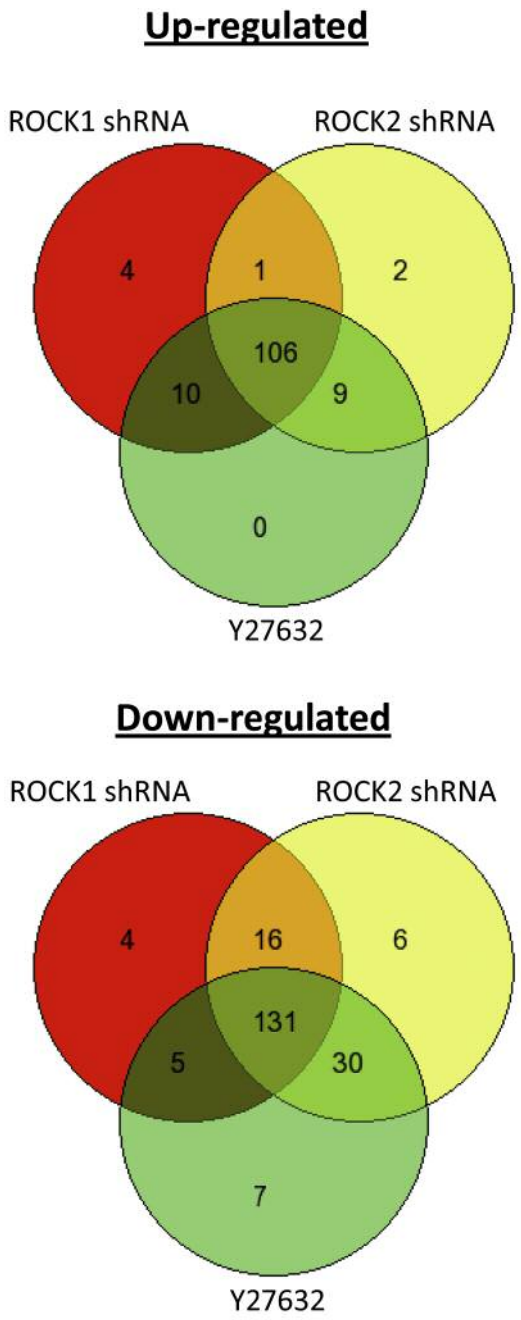

Figure 4. *Similarities in gene expression between each condition. Venn diagrams were generated for all miRNA gene expression changes altered by strictly greater than two-fold relative to the scrambled shRNA control.*

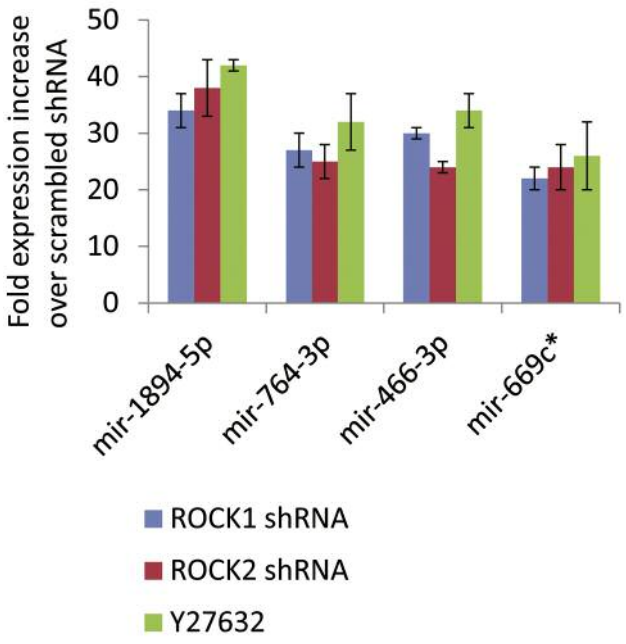

Figure 5. *Confirmation of microarray data. Confirmation of the microarray data by testing the steady-state expression levels of mir-1894-5p, mir-764-3p, mir-466f-3p, and mir-669c* in MS1 cells knocked-down for ROCK1 or ROCK2, or treated for 24 h with 10* μ*M Y27632 relative to the scrambled shRNA control.*

and Functional Study Database (MIRDB, www.mirdb.org) to identify 313, 188, 1052, and 1,670 statistically significant predicted targets for mir-1894-5p, mir-764-3p, mir-466f-3p, and mir-669c*, respectively. These gene lists were input into the Metacore integrated software suite for functional genomics and pathway analysis, revealing that a process network involving regulation of proliferation mostly characterized the predicted target genes for mir-1894-5p, including *Cx3crl, Adra1a, Nf1, Phb, Braf, Il1r1, Gpnmb, Dlg3, Igfbp5, Tob2*. mir-764-3p predicted target genes were mostly characterized by a process network involving in calcium transport (*Grik3, Atp2b4, Atp2a2, Otof, Trpc3, Ydr*). mir-466f-3p-predicted target genes were most characterized by a process network involving G1/S cell-cycle regulation (*Tcf7l2, Akt3, Prkcd, Prkc1, Pdgfra, Grb2, Cbl, Rbm5, Cdkn1b, Sos1, Sos2, Rgl2, Gsk3b, Pik3ca, Pik3rl, Igflr, Rbl2, Tgfbr1, Gnai, Jun, Stat5b*). mir-669c*-predicted target genes were most characterized by a process network involving neurogenesis and synaptogenesis (*Wnt5a, Klk6, Fzd4, Fzd5, Fzd3, Fzd9, Lrp8, Prkca, Stc16, Vamp1, Vamp2, Agrn, Fgf5, Frs2, Sntb2, Apba1, Syt2, Syt13, Syt7, Syt4, Pclo, Bsn, Erc2, Shc1, Sema4c, Trpc5, Kcnq2*). As an independent analysis of the strength of the known direct and indirect functional interactions between the predicted target genes for each miRNA, we input each gene list into the Search Tool for the Retrieval of Interacting Genes/Proteins (String, www.string-db.org). A moderate number of functional interactions between predicted gene targets is observed for *mir-1894-5p* and *mir-764-3p*, and a very large cluster of functional interactions is evident for *mir-466-3p* and *mir-669-c** (data not shown).

Table II. *Fold change in miRNA expression as a result of shRNA-mediated ROCK-knockdown or pharmacological inhibition of ROCK activity.*

miRNA Symbol	ROCK1 shRNA *vs*. control	ROCK2 shRNA *vs*. control	Y27632 *vs*. control
mmu-miR-1894-5p	308.08	207.41	558.9
mmu-miR-466f-3p	116.88	91.7	402.89
mmu-miR-764-3p	99.48	63.96	106.17
mmu-miR-669c*	76.26	67.27	140.81
mmu-miR-149*	56.24	33.7	20.24
mmu-miR-764-5p	52.89	12.74	13.35
mmu-miR-665	47.02	20	25.57
mmu-miR-3102*	44.23	21.6	24.54
mmu-miR-705	34.97	9.7	38.97
mmu-miR-802*	34.52	17.71	29.83
mmu-miR-669d	29.02	25.65	41.34
mmu-miR-92b*	28.44	34.39	27.56
mmu-miR-667	26.73	5.2	6.08
mmu-miR-504*	26.71	5.02	6.11
mmu-miR-210*	23.56	13.5	26.76
mmu-miR-1952	22.93	14.63	42.03
m-73B	21.53	19.94	20.42
mmu-miR-467h	20.86	28.06	23.96
mmu-miR-872	20.42	20.98	14.91
mmu-miR-883a-5p	19.67	23.38	26.63
mmu-miR-1188*	19.42	6.23	6.45
mmu-miR-1894-3p	18.56	5.91	19.43
mmu-miR-296-3p	17.52	6.7	6.6
mmu-miR-1949	17.09	–0.54	0.39
mmu-miR-494	16.61	3.41	6.01
mmu-miR-5128	16.58	7.79	6.6
mmu-miR-5132	16.3	10.55	16.07
mmu-miR-669l*	16.21	13.74	35.31
mmu-miR-210	16.14	–0.02	2.08
mmu-miR-2183	16.13	11.11	31.26
mmu-miR-720	15.66	37.01	27.79
mmu-miR-1892	14.7	7.58	6.66
mmu-miR-1247*	14.6	2.85	4.11
mmu-miR-1224*	14.02	13.35	6.69
mmu-miR-714	13.88	16.16	24.9
mmu-miR-874*	13.86	5.48	12.03
mmu-miR-1187	13.17	8.58	21.48
mmu-miR-762	12.96	4.09	7.79
mmu-miR-1943*	11.99	7.7	15.06
mmu-miR-5127	11.84	13.9	20.48
mmu-let-7a	11.73	4.46	5.77
mmu-miR-3102-3p.2	11.5	5.38	14.79
mmu-miR-760-5p	11.21	4.97	10.82
mmu-miR-320	11.12	3.3	2.18
mmu-miR-466q	10.47	4.45	4.46
mmu-miR-664	10.35	7.01	30.99
mmu-miR-5109	10.26	6.73	12
mmu-miR-5105	10.08	1.3	2.51
mmu-miR-207	9.96	5.32	12.77
mmu-miR-3473d	9.61	1.67	6.36
mmu-miR-1940	9.5	7.29	15.16
mmu-miR-3960	8.9	1.5	2.12
mmu-miR-667*	8.66	2.55	3.33
mmu-miR-3473b	8.57	2.93	5.19
mmu-miR-1249*	8.51	4.73	3.02
mmu-miR-92a-2*	8.36	4.6	7.22
mmu-miR-669f-5p	7.79	4.76	5.21
mmu-miR-5115	7.75	9.29	9.66
mmu-miR-328*	6.92	6.45	6.02
mmu-miR-877*	6.87	8.92	39.53
mmu-miR-3100-5p	6.55	0.56	3.24
mmu-miR-466f-5p	6.27	2.69	7.13
mmu-miR-346*	5.97	3.01	2.71
mmu-miR-32*	5.9	1.84	4.21
mmu-miR-5110	5.57	6.07	10.68
mmu-miR-7b*	5.34	3.45	7.04
mmu-miR-3090*	5.23	2.88	2.43
mmu-miR-18b*	5.2	4.69	9.14
mmu-miR-669p*	5.08	3	9.24
mmu-miR-466k	4.96	2.71	2.35
mmu-miR-1930	4.89	–0.88	0.46
mmu-miR-466i-3p	4.84	2.27	5.16
mmu-miR-466f	4.76	3.91	4.92
mmu-miR-709	4.61	2.58	3.91
mmu-miR-669n	4.6	2.2	4.52
mmu-miR-466h-3p	4.53	3.75	10.37
mmu-miR-3082-5p	4.47	2.98	8.42
mmu-miR-466j	4.42	2.72	5.93
mmu-miR-3057-3p	4.38	6.45	4.29
mmu-miR-3076-5p	4.09	2.08	2.09
mmu-miR-150	3.94	2.81	2.69
mmu-miR-5126	3.82	4.04	4.78
mmu-miR-1897-5p	3.81	5.51	5.47
mmu-miR-466c-5p	3.73	2.8	4.7
mmu-miR-30c-1*	3.65	3.62	7.26
mmu-miR-466b-5p, mmu-miR-466o-5p	3.43	2.54	3.39
mmu-miR-211*	3.42	1.24	3.44
mmu-miR-5107	3.37	2.31	5.96
mmu-miR-3099	3.34	2.05	2.25
mmu-let-7e	3.24	3.1	3.55
mmu-miR-455	3.22	2.15	–1.55
mmu-miR-468	3.21	4.5	5.6
mmu-miR-574-5p	3.17	4.17	6.3
mmu-miR-2182	3.17	2.21	3.98
mmu-miR-698	3.09	4.9	3.19
mmu-miR-3099*	3.01	2.34	4.13
mmu-miR-672	2.92	5.29	5
mmu-miR-2137	2.9	3.45	2.65
mmu-miR-466m-3p	2.77	3.43	6.26
mmu-miR-328	2.77	1.93	3.18
mmu-miR-1192	2.76	3.41	4.87
mmu-miR-5099	2.73	4.26	3.92
mmu-miR-3107, mmu-miR-486	2.71	2.2	3.43
mmu-miR-222*	2.7	–3.45	–1.9
mmu-miR-3103	2.66	1.55	2.22
mmu-miR-483	2.65	5.15	6.41
mmu-miR-3968	2.63	3.95	3.42
mmu-miR-3473	2.62	2.29	5.4
mmu-miR-1902	2.55	2.28	6.63
mmu-miR-669k*	2.42	3.44	5.34
mmu-miR-669o-5p	2.42	3.43	2.73

Table II. *Continued*

Table II. *Continued*

miRNA Symbol	ROCK1 shRNA *vs*. control	ROCK2 shRNA *vs*. control	Y27632 *vs*. control
mmu-miR-3070a*, mmu-miR-3070b-5p	2.32	2.21	2.56
mmu-miR-5136	2.28	4.94	3.73
mmu-miR-1196	2.28	1.36	3.34
mmu-miR-3087*	2.26	3.58	3.55
mmu-miR-669b	2.2	2.52	2.78
mmu-miR-664*	2.14	2.74	3.53
mmu-miR-208b*	2.01	–8.61	–3.48
mmu-miR-194	1.98	–11.54	–4.01
mmu-miR-702	1.96	3.39	6.12
mmu-miR-29b-1*	1.88	2.12	3.51
mmu-miR-1249	1.86	2.36	2.03
mmu-miR-1934*	1.83	2.9	2.22
mmu-miR-3064-5p	1.82	2.03	2.27
mmu-miR-669d*, mmu-miR-669d-2*	1.69	2.51	5.09
mmu-miR-568	1.46	–44.67	–3.84
mmu-miR-669a-3-3p	1.25	2.19	2.46
mmu-miR-135b*	0.99	–3.89	–2.33
mmu-miR-666-3p	0.91	–32.22	–6.2
mmu-miR-3070b-3p	0.53	3.03	2.49
mmu-miR-344e*	0.46	3.54	1.48
mmu-miR-499	–0.35	–2.73	–23.46
mmu-miR-199b*	–0.36	–6.46	–16.46
mmu-miR-376c	–0.54	–52.35	–5.13
mmu-miR-329	–0.62	–1.01	–3.74
mmu-miR-186	–0.66	–7.11	–7.55
mmu-miR-148a	–0.69	–29.17	–4.66
mmu-miR-344	–0.72	–5.96	–8
mmu-miR-340-5p	–0.78	–3.87	–7.16
mmu-miR-590-3p	–0.91	–36.27	–34.53
mmu-miR-708	–0.97	–6.37	–5.78
mmu-miR-221*	–1	–3.79	–6.05
mmu-miR-294*	–1.03	–3.2	–2.4
mmu-miR-598	–1.05	5.27	0.97
mmu-miR-449b	–1.21	–2.48	–2.23
mmu-miR-878-5p	–1.25	–2.62	–31.61
mmu-miR-708*	–1.29	–23.99	–13.68
mmu-miR-1251*	–1.37	–4.6	–2.44
mmu-miR-103-2*	–1.54	–1.41	–10.78
mmu-miR-1901	–1.58	–2.23	0.24
mmu-miR-185	–1.6	–44.89	–2.79
mmu-miR-130a*	–1.64	–2.94	0.39
mmu-miR-3086-3p	–1.64	–4.43	–3.62
mmu-miR-1b-3p	–1.68	–29.77	–2.48
mmu-miR-217	–1.72	–1.21	–4.08
mmu-miR-1953	–1.73	1.72	–2.1
mmu-miR-376a	–1.74	–1.5	–22.87
mmu-miR-433*	–1.75	0.41	–4.8
mmu-miR-362-3p	–1.76	–2.99	–0.66
mmu-miR-203*	–1.76	–3.18	–2.21
mmu-miR-669j	–1.77	–2.31	–2.6
mmu-miR-490-5p	–1.8	–2.94	–2.25
mmu-miR-491*	–1.83	–6.15	–3.14
mmu-miR-127	–1.85	–2.53	–1.22
mmu-miR-204	–1.89	–27.74	–15.22
mmu-let-7i*	–1.91	–3.34	–16.23
mmu-miR-10b	–1.95	–2.33	–2.18
mmu-miR-3110*	–1.96	–4.55	–1.81
mmu-miR-196a	–1.97	–0.65	–4.97
mmu-miR-876-5p	–2.08	–2.32	–2.82
mmu-miR-376c*	–2.08	–5.47	–1.7
mmu-miR-592*	–2.09	–20.06	–2.91
mmu-miR-367	–2.1	–39.8	–1.52
mmu-miR-34a*	–2.15	–19.35	–11.88
mmu-miR-547	–2.16	–42.81	–3.66
mmu-miR-135b	–2.18	–11.29	–6.72
mmu-miR-1198-3p	–2.19	–4.8	–12.06
mmu-miR-3067	–2.19	–22.19	–0.9
mmu-miR-29a	–2.23	–1.54	–1.34
mmu-miR-154	–2.23	–3.16	–1.69
mmu-miR-183	–2.25	–3.47	–2.56
mmu-miR-3109*	–2.26	–3.05	–2.33
mmu-miR-135a	–2.28	–2.3	–48.7
mmu-miR-128	–2.29	–1.8	–1.72
mmu-miR-26a-1*	–2.3	–7.86	–2.55
mmu-miR-1298	–2.32	–2.3	–1.16
mmu-miR-411*	–2.45	–2.61	–3.17
mmu-miR-293	–2.45	–46.74	–4.95
mmu-miR-195	–2.5	–0.46	–1.87
mmu-miR-124*	–2.53	–2.94	–4.75
mmu-miR-18a*	–2.54	–2.19	–3
mmu-miR-374, mmu-miR-374c	–2.54	–3.72	–1.42
mmu-miR-96*	–2.55	–0.66	–10.47
mmu-miR-103-1*	–2.55	–2.98	–1.87
mmu-miR-551b	–2.55	–6.47	–5.96
mmu-miR-34b-5p	–2.59	–35.53	–2.27
mmu-miR-335-5p	–2.61	–3.1	–20.64
mmu-miR-126-5p	–2.65	–2.53	–2.03
mmu-miR-495	–2.67	–2.63	–11.87
mmu-miR-154*	–2.69	–2.34	–3.23
mmu-miR-200b*	–2.7	–2.2	–2.28
mmu-miR-146a*	–2.7	–2.43	–2.37
mmu-miR-669k	–2.78	–4.48	–6.56
mmu-miR-326	–2.79	–3.25	–1.46
mmu-miR-193	–2.8	–2.52	–14.58
mmu-miR-344e	–2.8	–11.2	–5.55
mmu-miR-193b	–2.81	–4.6	–5.69
mmu-miR-382*	–2.82	–39.35	–0.12
mmu-miR-759	–2.86	–16.72	–1.9
mmu-miR-433	–2.87	–3.2	–4.36
mmu-miR-181a-2*	–2.92	–2.5	–7.65
mmu-miR-487b	–2.93	–5.79	–5.1
mmu-miR-20a*	–2.93	–38.04	–1
mmu-miR-592	–2.98	–3.23	–13.74
mmu-miR-217*	–3.03	–6.37	–2.67
mmu-miR-205	–3.06	–5.3	–2.5
mmu-miR-470*	–3.08	–5.84	–2.27
mmu-miR-1932	–3.1	–2.55	–11.76
mmu-miR-1193-3p	–3.11	–2.78	–5.8
mmu-miR-684	–3.14	–4.71	–1.77
mmu-miR-96	–3.17	–4.36	–2.02
mmu-miR-139-3p	–3.18	–9.54	–1.36
mmu-miR-1264-5p	–3.24	–20.1	–10.35
mmu-miR-741*	–3.27	0.77	–7.03

Table II. *Continued*

Table II. *Continued*

miRNA Symbol	ROCK1 shRNA *vs*. control	ROCK2 shRNA *vs*. control	Y27632 *vs*. control
mmu-miR-466a-3p, mmu-miR-466b-3p, mmu-miR-466c-3p, mmu-miR-466e-3p, mmu-miR-466p-3p	–3.29	–3.62	–2.73
mmu-miR-133a*	–3.33	–1.73	–1.11
mmu-miR-101b*	–3.37	–4.44	–15.12
mmu-miR-1199	–3.37	–5.7	–4.45
mmu-miR-331-5p	–3.38	–2.45	–2.6
mmu-miR-1955-5p	–3.45	–174.68	–1.08
mmu-miR-301b	–3.46	–6.35	–9.12
mmu-miR-3970	–3.47	–2.07	–12.77
mmu-miR-471-3p	–3.55	–2.6	–3.77
mmu-miR-24-2*	–3.57	–4.21	–9.84
mmu-miR-3071*	–3.67	–4.51	–3.36
mmu-miR-181a-1*	–3.68	–0.86	–4.44
mmu-miR-100	–3.72	–3.62	–1.71
mmu-miR-5103	–3.74	–6.08	–3.02
mmu-miR-463*	–3.83	–4.53	–5.17
mmu-miR-3088	–3.87	–3.99	–3.05
mmu-miR-19a*	–3.91	–1.4	–37.2
mmu-miR-122*	–3.92	–5.33	–2.93
mmu-miR-3112	–4	–40.83	–5.76
mmu-miR-130b*	–4.03	–12.59	–34.42
mmu-miR-882	–4.08	–4.14	–2.18
mmu-miR-30a	–4.1	–31.41	–4.65
mmu-miR-384-3p	–4.12	–4.87	–46.42
mmu-miR-148b*	–4.13	–2.44	–14.38
mmu-miR-879	–4.28	–22.64	–12.8
mmu-miR-202-5p	–4.43	–115.03	–43.57
mmu-miR-1a	–4.49	–1.68	–2.43
mmu-miR-139-5p	–4.49	–5.47	–3.75
mmu-miR-28b	–4.64	–4.33	–2.51
mmu-miR-181b	–4.7	–6.73	–3.21
mmu-miR-196a-2*	–4.74	–9.21	–7.77
mmu-miR-30b	–4.76	–20.67	–3.94
mmu-miR-208b	–4.87	–4.45	–5.73
mmu-miR-137	–4.87	–6.01	–2.35
mmu-miR-3471	–4.95	–5.45	–3.7
mmu-miR-299	–4.98	–12.47	–2.75
mmu-miR-1968*	–5.02	–79.22	–5.07
mmu-miR-3078*	–5.19	–3.87	–20.1
mmu-miR-543	–5.19	–10.51	–83.02
mmu-miR-295	–5.29	–22.55	–14.62
mmu-miR-1264-3p	–5.3	–9.41	–50.19
mmu-miR-301b*	–5.35	–5.97	–5.24
mmu-miR-133b	–5.44	–9.49	–4.94
mmu-miR-3075*	–5.6	–9.69	–13.74
mmu-miR-378	–5.62	–5.95	–5.06
mmu-miR-500*	–5.92	–3.63	–6.73
mmu-miR-201	–6.07	–20.05	–40.05
mmu-miR-203	–6.11	–12.1	–3.5
mmu-miR-3083	–6.25	–4.99	–6.61
mmu-miR-496	–6.28	–26.22	–5.44
mmu-miR-871-5p	–6.37	–8.6	–3.57
mmu-miR-155*	–6.54	–33.12	–19.24
mmu-miR-219-3p	–6.61	–5.34	–10.93
mmu-miR-450a-1*	–6.75	–4.7	–2.57
mmu-miR-379*	–6.82	–9.03	–3.36
mmu-miR-3095-5p	–7.04	–7.13	–23.53
mmu-miR-384-5p	–7.13	–46.87	–26.1
mmu-miR-138-2*	–7.14	–9.65	–4.34
mmu-let-7f-2*	–7.24	–28.33	–7.13
mmu-miR-3092*	–7.47	–63.03	–12.19
mmu-miR-144*	–7.49	–14.47	–3.54
mmu-miR-184	–7.6	–3.18	–6.9
mmu-miR-1194	–7.93	–5.37	–44.56
mmu-miR-802	–8.11	–124.93	–6.99
mmu-miR-19b-1*	–8.46	–268.29	–6.85
mmu-miR-26a	–8.54	–251.39	–4.51
mmu-miR-99a	–8.65	–7.82	–3.13
mmu-miR-3962	–8.87	–35.99	–8.33
mmu-miR-130b	–9.3	–5.25	–5.88
mmu-miR-676*	–9.72	–6.86	–6.01
mmu-miR-3965	–9.92	–3.11	–7.67
mmu-miR-323-3p	–10.17	–33.2	–20.6
mmu-miR-153	–10.34	–156.04	–19.87
mmu-miR-484	–10.38	–6.61	–3.35
mmu-miR-3066	–10.39	–57.28	–7.65
mmu-miR-145*	–10.48	–12.12	–5.29
mmu-let-7d*	–11.23	–13.49	–7.81
mmu-miR-140	–11.35	–3.87	–12.26
mmu-miR-1251	–11.59	–78.84	–88.87
mmu-miR-24-1*	–13.57	–118.07	–17.02
mmu-miR-142-5p	–13.84	–15.14	–11.78
mmu-miR-1843-5p	–14.56	–7.14	–14.11
mmu-miR-463	–14.79	–16.48	–12.24
mmu-miR-1928	–14.87	–28.84	–29.96
mmu-miR-190*	–18.68	–105.99	–121.41
mmu-miR-582-5p	–19.79	–54.34	–46.68
mmu-miR-1965	–20.29	–42.26	–24.35
mmu-miR-467d	–20.67	–53.45	–6.4
mmu-miR-218-2*	–21.06	–41.18	–14.81
mmu-miR-26b	–22.4	–104.74	–16.06
mmu-miR-302b*	–23.01	–12.34	–7.33
mmu-miR-224	–28.7	–152.47	–19.28
mmu-miR-505-3p	–30.69	–24.97	–15.31
mmu-miR-471-5p	–34.21	–2.7	–11.53
mmu-miR-448-3p	–38.49	–2.19	–4.4
mmu-miR-302c*	–46.79	–39.42	–6.46

Discussion

A previously published comparative miRNA expression analysis of endothelial cells from the aorta, coronary artery, umbilical vein, pulmonary artery, pulmonary microvasculature, dermal microvasculature, and brain microvasculature revealed 166 miRNAs expressed in the panel of endothelial cells (20). While many of these miRNAs

were shared with endothelial, epithelial, and hematological cells, 31 miRNAs were markers solely of endothelial cells. Our analysis of the miRNA expression profiles in MS1 endothelial cells tested a significantly larger panel of miRNAs than McCall *et al*. (20). Out of the miRNAs reportedly expressed across endothelial cells by these authors, we were able to corroborate the expression of approximately 50% of these in our analysis, suggesting that tumor-forming endothelial lines share somewhat similar expression patterns with other endothelial cells, but to a large degree reflect a unique miRNA profile.

RhoA/ROCK signaling has been implicated in a plethora of diverse cellular processes, and there is little doubt based on published literature that these proteins induce significant alterations in global gene expression. These expression changes may either occur through direct interactions of the ROCK proteins with a host of downstream transcriptional regulators (21) or *via* indirect actin-cytoskeleton-mediated regulation of transcription, through altering the mechanical properties of the cell (22, 23). Indeed, our laboratory has previously reported that shRNA-knockdown of ROCK1 or ROCK2, as well as Y27632 treatment of endothelial cells induces large-scale changes in mRNA expression (4). We demonstrated that many of these downstream transcription effects were shared between ROCK1 and ROCK2, however a large number was unique to either of the paralogs, suggesting that these proteins have both overlapping and distinct roles in transcriptional regulation. Furthermore, ROCK-knockdown is capable of ablating approximately half of all vascular endothelial growth factor (VEGF)-stimulated transcriptional regulation (4), indicating that ROCK signaling is critical for vascular physiology given the central importance of VEGF signaling in blood vessels. While *ROCK* mRNAs have been shown to be targeted by miRNA-mediated degradation (24-28), little is known regarding the effects of ROCK signaling on miRNA global expression. Liu *et al*. demonstrated that treatment of MCF7 breast cancer cells with Y27632 or ROCK-targeting siRNAs reduces cell migration, cell proliferation, and bone metastasis, in part, *via* a down-regulation of the c-Myc-regulated mir-17-92 cluster (15). Beyond this study, the regulation of miRNAs by these central regulators is unknown. Our data reveal that approximately one third of the miRNAs that were tested in our experiments exhibited altered expression levels in the ROCK knockdowns and Y27632 treatment, suggesting that similar to the dramatic ROCK-mediated mRNA expression previously reported, ROCK proteins induce large-scale and substantial changes in miRNA gene expression (4). Given that ROCK proteins are major modulators of cellular shape (29), our findings are not surprising considering that alterations in cellular shape have been shown to alter the expression patterns of approximately 10% of the protein-coding genome, and, as our data indicate, this logically extends to global miRNA expression patterns (23). Unlike the many instances of ROCK1- and ROCK2-specific regulation of mRNA gene expression that have been previously reported (4), our current data show that the two protein paralogs play almost completely overlapping roles in the global regulation of miRNA expression.

Out of the large number of miRNAs whose expression was altered following ROCK-knockdown or pharmacological inhibition, we focused our analysis on four miRNAs that were commonly up-regulated to a large degree in all treatments, including mir-1894-5p, mir-764-3p, mir-466f-3p, and mir-669c*. mir-1894 is a recently identified miRNA located close to retroviral integration sites and has been hypothesized to play a role in cell homeostasis (30). mir-466f-3p is located in the first intron of the *COL3A1* gene and is predicted to regulate the expression of several collagen genes during development (31). Furthermore, this miRNA has been shown to be overexpressed in streptozotocin-induced diabetic mouse models (32). mir-669c* is differentially expressed in a mouse model of Alzheimer's disease (33). To date, nothing has been reported regarding the function of mir-764-3p. Using a systems biology approach, we analyzed the potential functions of these four miRNAs revealing that their predicted target genes are significantly overrepresented by network processes involved in cell-cycle regulation (mir-1894-5p and mir-466f-3p), calcium transport (mir-764-3p), and neurogenesis and synaptogenesis (mir-669c*). ROCK signaling has been shown to dramatically affect cell-cycle progression through modulating the activity of a diverse array of downstream targets such as cyclins, cyclin-dependent kinases, cyclin-dependent kinase inhibitors, Ras/MAPK and many others (1). While many of these effects are likely mediated through direct phosphorylation of the target proteins by ROCK1 and ROCK2 (21), a large number of these reported regulations have not been demonstrated through direct protein-to-protein interactions. Thus, they may depend on the effects of the ROCK proteins on global transcription of mRNAs and particularly miRNAs such as mir-1894-5p and mir-466f-3p which we hypothesize to direct the stability of a number of transcripts involved in cell-cycle regulation. Calcium concentrations, prolactin, as well as glucose have been shown to activate RhoA/ROCK signaling pathways to modulate epithelial calcium transport (34-36). Furthermore, RhoA/ROCK activation is essential for calcium-regulated arterial contraction (37, 38). Despite the significant amount of evidence indicating that the RhoA/ROCK pathway is involved in calcium signaling, the mechanism controlling this process is completely unknown and may involve ROCK-mediated regulation of mir-764-3p which we hypothesize that it strongly regulates the levels of calcium transport genes. The amount of literature linking ROCK's kinase activity to neurite outgrowth and synaptogenesis is vast, and the use of Rho/ROCK inhibitors are emerging as effective strategies to

promote nerve re-generation following traumatic injury and target neurological disorders (39, 40). The overwhelming majority of this research is focused on the ability of ROCK to control cytoskeletal dynamics and subsequently modulate axon and dendrite growth and guidance. Interestingly, the predicted targets for mir-669c* are greatly over-represented by genes involved in neurogenesis and synaptogenesis and, as mentioned above, this miRNA has been shown to be differentially expressed in a neurodegenerative mouse model (33). Though our research utilized endothelial cells, if similar ROCK-mediated regulation of mir-669c* also occurs in neuronal cells, the effects of ROCK on neuronal cell structure and function may extend beyond simple regulation of the cytoskeleton.

Conclusion

Recent publications by our laboratory and others have shed light on the essential roles of ROCK signaling outside of the classical models, where ROCK1 and ROCK2 modulate actomyosin cytoskeleton contractility. The data presented in the present study expand those of our previous reports by providing strong evidence that ROCK signaling is essential for the steady-state expression of a large number of miRNAs in tumor-forming endothelial cells. These findings may open avenues for alternative therapeutic targeting of vascular diseases and cancer, not by directly targeting ROCK activity, but by inhibiting specific miRNAs that mediate ROCK-dependent processes.

Acknowledgements

This work was supported by a NIH NHLBI grant (HL098931) and a Liddy Shriver Sarcoma Initiative grant to BAB.

References

1 Street CA and Bryan BA: Rho kinase proteins – pleiotropic modulators of cell survival and apoptosis. Anticancer Res *31*: 3645-3657, 2001.

2 Rath N and Olson MF: Rho-associated kinases in tumorigenesis: re-considering ROCK inhibition for cancer therapy. EMBO Rep *13*: 900-908, 2012.

3 Bryan BA, Dennstedt E, Mitchell DC, Walshe TE, Noma K, Loureiro R, Saint-Geniez M, Campaigniac JP, Liao JK and D'Amore PA: RhoA/ROCK signaling is essential for multiple aspects of VEGF-mediated angiogenesis. FASEB J *24*: 3186-3195, 2010.

4 Montalvo J, Spencer C, Hackathorn A, Masterjohn K, Perkins A, Doty C, Arumugam A, Ongusaha PP, Lakshmanaswamy R, Liao JK, Mitchell DC and Bryan BA: ROCK1 & 2 perform overlapping and unique roles in angiogenesis and angiosarcoma tumor progression. Curr Mol Med *13*: 205-219, 2013.

5 Bryan BA and D'Amore PA: What tangled webs they weave: Rho-GTPase control of angiogenesis. Cell Mol Life Sci *64*: 2053-2065, 2007.

6 Mavria G, Vercoulen Y, Yeo M, Paterson H, Karasarides M, Marais R, Bird D and Marshall CJ: ERK-MAPK signaling opposes Rho-kinase to promote endothelial cell survival and sprouting during angiogenesis. Cancer Cell *9*: 33-44, 2006.

7 Yin L, Morishige K, Takahashi T, Hashimoto K, Ogata S, Tsutsumi S, Takata K, Ohta T, Kawagoe J, Takahashi K and Kurachi H: Fasudil inhibits vascular endothelial growth factor-induced angiogenesis *in vitro* and *in vivo*. Mol Cancer Ther *6*: 1517-1525, 2007.

8 Hata Y, Miura M, Nakao S, Kawahara S, Kita T and Ishibashi T: Antiangiogenic properties of fasudil, a potent Rho-Kinase inhibitor. Jpn J Ophthalmol *52*: 16-23, 2008.

9 Ghosh K, Thodeti CK, Dudley AC, Mammoto A, Klagsbrun M and Ingber DE: Tumor-derived endothelial cells exhibit aberrant Rho-mediated mechanosensing and abnormal angiogenesis *in vitro*. Proc Natl Acad Sci USA *105*: 11305-11310, 2008.

10 Mammoto A, Mammoto T and Ingber DE: Mechanosensitive mechanisms in transcriptional regulation. J Cell Sci *125*: 3061-3073, 2012.

11 Spencer C, Montalvo J, McLaughlin SR and Bryan BA: Small molecule inhibition of cytoskeletal dynamics in melanoma tumors results in altered transcriptional expression patterns of key genes involved in tumor initiation and progression. Cancer Genomics Proteomics *8*: 77-85, 2011.

12 Berenjeno IM and Bustelo XR: Identification of the Rock-dependent transcriptome in rodent fibroblasts. Clin Transl Oncol *10*: 726-738, 2008.

13 Boerma M, Fu Q, Wang J, Loose DS, Bartolozzi A, Ellis JL, McGonigle S, Paradise E, Sweetnam P, Fink LM, Vozenin-Brotons MC and Hauer-Jensen M: Comparative gene expression profiling in three primary human cell lines after treatment with a novel inhibitor of Rho kinase or atorvastatin. Blood Coagul Fibrinolysis *19*: 709-718, 2008.

14 Harvey SA, Anderson SC and SundarRaj N: Downstream effects of ROCK signaling in cultured human corneal stromal cells: microarray analysis of gene expression. Invest Ophthalmol Vis Sci *45*: 2168-2176, 2004.

15 Liu S, Goldstein RH, Scepansky EM and Rosenblatt M: Inhibition of rho-associated kinase signaling prevents breast cancer metastasis to human bone. Cancer Res *69*: 8742-8751, 2009.

16 Ishizaki T, Uehata M, Tamechika I, Keel J, Nonomura K, Maekawa M and Narumiya S: Pharmacological properties of Y-27632, a specific inhibitor of rho-associated kinases. Mol Pharmacol *57*: 976-983, 2000.

17 Pirooznia M, Nagarajan V and Deng Y: GeneVenn – A web application for comparing gene lists using Venn diagrams. Bioinformation *1*: 420-422, 2007.

18 Zhang B, Pan X, Cobb GP and Anderson TA: microRNAs as oncogenes and tumor suppressors. Dev Biol *302*: 1-12, 2007.

19 Arbiser JL, Moses MA, Fernandez CA, Ghiso N, Cao Y, Klauber N, Frank D, Brownlee M, Flynn E, Parangi S, Byers HR and Folkman J: Oncogenic H-ras stimulates tumor angiogenesis by two distinct pathways. Proc Natl Acad Sci USA *94*: 861-866, 1997.

20 McCall MN, Kent OA, Yu J, Fox-Talbot K, Zaiman AL and Halushka MK: MicroRNA profiling of diverse endothelial cell types. BMC Med Genomics *4*: 78, 2011.

21 Nishioka T, Nakayama M, Amano M and Kaibuchi K: Proteomic screening for Rho-kinase substrates by combining kinase and phosphatase inhibitors with 14-3-3zeta affinity chromatography. Cell Struct Funct *37*: 39-48, 2012.

22 Jain N, Iyer KV, Kumar A and Shivashankar GV: Cell geometric constraints induce modular gene-expression patterns *via* redistribution of HDAC3 regulated by actomyosin contractility. Proc Natl Acad Sci USA *110*: 11349-11354, 2013.
23 Stiles JM, Pham R, Rowntree RK, Amaya C, Battiste J, Boucheron LE, Mitchell DC and Bryan BA: Morphological restriction of human coronary artery endothelial cells substantially impacts global gene expression patterns. FEBS J *280*: 4474-4494, 2013.
24 Jiang L, Liu X, Kolokythas A, Yu J, Wang A, Heidbreder CE, Shi F and Zhou X: Down-regulation of the Rho GTPase signaling pathway is involved in the microRNA-138-mediated inhibition of cell migration and invasion in tongue squamous cell carcinoma. Int J Cancer *127*: 505-512, 2010.
25 Wong CC, Wong CM, Tung EK, Au SL, Lee JM, Poon RT, Man K and Ng IO: The microRNA miR-139 suppresses metastasis and progression of hepatocellular carcinoma by down-regulating Rho-kinase 2. Gastroenterology *140*: 322-331, 2011.
26 Ueno K, Hirata H, Shahryari V, Chen Y, Zaman MS, Singh K, Tabatabai ZL, Hinoda Y and Dahiya R: Tumour suppressor microRNA-584 directly targets oncogene Rock-1 and decreases invasion ability in human clear cell renal cell carcinoma. Br J Cancer *104*: 308-315, 2011.
27 Zheng B, Liang L, Wang C, Huang S, Cao X, Zha R, Liu L, Jia D, Tian Q, Wu J, Ye Y, Wang Q, Long Z, Zhou Y, Du C, He X and Shi Y: MicroRNA-148a suppresses tumor cell invasion and metastasis by downregulating ROCK1 in gastric cancer. Clin Cancer Res *17*: 7574-7583, 2011.
28 Cimino D, De Pitta C, Orso F, Zampini M, Casara S, Penna E, Quaglino E, Forni M, Damasco C, Pinatel E, Ponzone R, Romualdi C, Brisken C, De Bortoli M, Biglia N, Provero P, Lanfranchi G and Taverna D: miR148b is a major coordinator of breast cancer progression in a relapse-associated microRNA signature by targeting ITGA5, ROCK1, PIK3CA, NRAS, and CSF1. FASEB J *27*: 1223-1235, 2013.
29 Amano M, Nakayama M and Kaibuchi K: Rho-kinase/ROCK: A key regulator of the cytoskeleton and cell polarity. Cytoskeleton (Hoboken) *67*: 545-554, 2010.
30 Huppi K, Pitt J, Wahlberg B and Caplen NJ: Genomic instability and mouse microRNAs. Toxicol Mech Methods *21*: 325-333, 2011.
31 Sterling KM: The procollagen type III, alpha 1 (COL3A1) gene first intron expresses poly-A+ RNA corresponding to multiple ESTs and putative miRNAs. J Cell Biochem *112*: 541-547, 2011.
32 Chen YQ, Wang XX, Yao XM, Zhang DL, Yang XF, Tian SF and Wang NS: Abated microRNA-195 expression protected mesangial cells from apoptosis in early diabetic renal injury in mice. J Nephrol *25*: 566-576, 2012.
33 Ding Y, Tian M, Liu J, Deng Y, Li W, Feng X and Hou D: Expression profile of miRNAs in APP swe/PSDeltaE9 transgenic mice. Nan Fang Yi Ke Da Xue Xue Bao *32*: 1280-1283, 2012.
34 Samarin SN, Ivanov AI, Flatau G, Parkos CA and Nusrat A: Rho/Rho-associated kinase-II signaling mediates disassembly of epithelial apical junctions. Mol Biol Cell *18*: 3429-3439, 2007.
35 Thongon N, Nakkrasae LI, Thongbunchoo J, Krishnamra N and Charoenphandhu N: Prolactin stimulates transepithelial calcium transport and modulates paracellular permselectivity in Caco-2 monolayer: mediation by PKC and ROCK pathways. Am J Physiol Cell Physiol *294*: C1158-1168, 2008.
36 Cazzola M, Calzetta L, Rogliani P, Lauro D, Novelli L, Page CP, Kanabar V and Matera MG: High glucose enhances responsiveness of human airways smooth muscle *via* the Rho/ROCK pathway. Am J Respir Cell Mol Biol *47*: 509-516, 2012.
37 Fernandez-Tenorio M, Porras-Gonzalez C, Castellano A, Lopez-Barneo J and Urena J: Tonic arterial contraction mediated by L-type Ca^{2+} channels requires sustained Ca^{2+} influx, G protein-associated Ca^{2+} release, and RhoA/ROCK activation. Eur J Pharmacol *697*: 88-96, 2012.
38. Martinsen A, Yerna X, Rath G, Gomez EL, Dessy C and Morel N: Different effect of Rho kinase inhibition on calcium signaling in rat isolated large and small arteries. J Vasc Res *49*: 522-533, 2012.
39 Kubo T and Yamashita T: Rho-ROCK inhibitors for the treatment of CNS injury. Recent Pat CNS Drug Discov *2*: 173-179, 2007.
40 Mueller BK, Mack H and Teusch N: Rho kinase, a promising drug target for neurological disorders. Nat Rev Drug Discov *4*: 387-398, 2005.

Received October 29, 2013
Revised December 3, 2013
Accepted December 4, 2013